Korean J. Chem. Eng., 40(2), 405-411 (2023)
DOI: 10.1007/s11814-022-1288-8

pISSN: 0256-1115
eISSN: 1975-7220

Chitosan/oleamide blended electrospun nanofiber with enhanced spinnability and moderate hydrophobicity

Eunjoo Moon*,‡, Eungsu Kang*,‡, Wooho Song*, Bum Jin Kim, Hyung Joon Cha**, and Yoo Seong Choi*,†**

*Department of Chemical Engineering and Applied Chemistry, Chungnam National University, Daejeon 34134, Korea
**Department of Chemical Engineering, Pohang University of Science and Technology, Pohang 37673, Korea
(*Received 25 July 2022 • Revised 6 September 2022 • Accepted 13 September 2022*)

Abstract−Chitosan-based nanofibers have become attractive biomaterials for wound healing and dressing applications based on their intrinsic biocompatibility, biodegradability, and antibacterial properties. However, the unstable spinnability of chitosan-based nanofibers has impeded further applications. In this paper, a fatty acid amide oleamide was used as a blending material for nanofiber fabrication. The addition of oleamide into chitosan moderately decreased the viscosity of the electrospinning solution, resulting in enhanced spinnability when constructing chitosan/oleamide blended nanofibers. Remarkably, the 1 : 0.5 ratio of chitosan/oleamide nanofibers exhibited relatively high hydrophobicity, decreased tensile strength, and increased elongation at break compared to chitosan-only nanofiber. The nanofiber showed similar and slightly higher cell adhesion in the *in vitro* cell culture with mouse preosteoblast MC3T3-E1 and fibroblast NIH/3T3 cells, respectively; however, the cell proliferation levels were decreased on the blended nanofiber surfaces, presumably due to their increased hydrophobicity. These results suggest that chitosan/oleamide nanofibers with high spinnability can be applied to the preparation of wound dressing membranes or patches with intrinsic antibacterial properties and moderate hydrophobicity. We expect that oleamide, which has lubricant and antibacterial properties, can be utilized as a blending component of chitosan-based nanofibers for biomaterial and tissue engineering applications.

Keywords: Biomaterial, Chitosan, Electrospinning, Nanofiber, Oleamide

INTRODUCTION

Electrospun nanofibers are considered to be versatile materials in various industrial fields, such as air purification technology, water treatment systems, catalytic supports, energy harvest/storage/conversion components, biomaterials, and tissue engineering applications [1,2]. Potential applications of electrospun nanofibers are based on the component materials' morphological, chemical, physical, and mechanical properties and the electrospinning procedure [1,3,4]. In particular, electrospun fibers that are structurally similar to natural extracellular matrices (ECMs) have been highly attractive for mimicking nanofibril structures in biomedical engineering applications [5,6]. ECM, as a noncellular 3-D biomolecular network, has various functional roles such as structural support and functional cellular regulation. ECMs are mainly composed of proteoglycans (PGs), glycosaminoglycans (GAGs), collagen, and other glycoproteins [7]. PGs and GAGs are primarily involved in the binding and assembly of growth factors and related biomolecules [8,9]. Polysaccharide-based natural biopolymers can act as versatile molecules for nanofibrous scaffold preparation due to their inherent biocompatible and biodegradable properties for biomedical applications, including wound dressing, drug delivery, and tissue engineering [10,11].

Among natural biopolymers, chitosan (CS) has been widely used for the preparation of nanofibrous scaffold materials since it is a naturally derived, biocompatible, and biodegradable biomaterial with structural and compositional similarity to GAGs [12,13]. Interestingly, CS has promising biological features for biomedical applications, including antibacterial and wound healing properties; the antibacterial properties can act as a physical barrier to prevent and kill invading microorganisms [14-16]. However, CS is dissolved in acidic media (pH<6) due to the positively charged amino groups that exist in this media, but it is nearly insoluble in water under physiological conditions, and its poor aqueous stability has somewhat limited its biomedical applications [13,17]. Moreover, because CS solutions become highly viscous and because the strong hydrogen bonds in a 3-D network prevent the movement of polymeric chains exposed to an electrical field, the electrospinning process of CS solutions is complicated [12,18]. In this manner, enhancing the processability of CS-based fibers has been comprehensively investigated for the construction of pristine fibrous mats [19,20].

Blending CS with other polymeric materials has become an attractive approach to enhance the mechanical and biological properties in a targeted manner [21,22]. Synthetic polymers have been found to mainly enhance mechanical and physicochemical properties of CS nanofibers, while natural polymers have been found to improve the biological activity of CS nanofibers. Remarkably, post-modification of CS nanofibers from fatty acids was found to effectively control the fibrous structure and enhance the stability of CS nanofibers in moist environments [17]. Essential oils and fatty acid derivatives were studied, and it was found that they could be

†To whom correspondence should be addressed.
E-mail: biochoi@cnu.ac.kr
‡These authors are equally contributed in this work.

loaded into nanofibers by electrospinning, which improved their antimicrobial, anti-inflammatory, antioxidant, and re-epithelialization properties [23,24]. In this manner, we recently found that the blending of oleamide (OA; $C_{18}H_{35}NO$), a fatty acid amide, with CS could improve the spinnability of the electrospinning process, which was successfully used for the construction of nanofluid components made from nanoparticles that enhance the gas utilization efficiency in C1-gas microbial biotransformation [25]. In our previous study, the addition of OA into CS solution enabled us to form stable nanoparticles that were well suspended in aqueous media [25]. As a fatty acid amide isolated from nature, OA could be a natural ingredient of antibacterial materials reducing frictional resistance or increasing lubricity when it acts as a lubricating agent [26,27].

In the present study, we constructed CS/OA blended electrospun nanofibers with various ratios of CS and OA. Viscosity measurements of the CS/OA mixture and morphological analyses of the constructed nanofibers enabled us to better understand the increased spinnability of the electrospinning process. Water contact angles and stress-strain curves displayed the wettability and mechanical properties of the CS/OA nanofiber mats. *In vitro* cell cultures using model mammalian cell lines, such as MC3T3-E1 and NIH/3T3, were performed to observe the early-stage cellular behavior on the CS/OA nanofiber scaffolds. The results showed that CS/OA blending could potentially be utilized in the preparation of nanofibrous biomaterials for biomedical applications.

EXPERIMENTAL

1. Preparation of CS/OA Blended Electrospun Nanofibers

CS (medium molecular weight: 190-310 kDa, deacetylation degree: 75-85%, and Brookfield viscosity: 200-800 cP), acetic acid, trifluoroacetic acid (TFA), 1,1,1,3,3,3-hexafluoro-2-propanol (HFIP), glutaraldehyde (GA), and ethanol (EtOH) were purchased from Sigma-Aldrich Inc., MA, USA. OA was purchased from J&H Chemical Co., China. The CS/OA fibers were fabricated by an electrospinning process after the preparation of CS/OA blended solutions with different mixing ratios. The solutions were prepared by dissolving 0.5 g of CS and 0-2 g of OA in 6.5 mL of TFA and HFIP cosolvent at 44-50 °C for 10 min and then by mixing at 80-110 rpm with a 1.5 cm axial diameter magnetic stirrer for 12 hr at 30 °C. The CS/OA solution was electrospun from a 6 mL plastic syringe (Restek Co., PA, USA) with a 12.46 mm metal syringe needle (Nano-NC Co., South Korea) and an electrospinning apparatus (Nano-NC Co., South Korea). The CS/OA fiber was collected on aluminum foil under the conditions of 25-28 °C temperatures and 40-60% relative humidity; 24-26 kV voltage was supplied at the tip and needle, and the mass flow rate of the solution was set at 0.35 mL/hr. The fiber was dried in a vacuum-dry oven (Jeio Tech Ltd., South Korea) for at least 24 hours to evaporate the remaining solvents. The dried CS/OA fiber was crosslinked for 24 hours in polypropylene desiccators filled with 1 mL of 75% (v/v) GA solution. Finally, the sample was dried at 40 °C for 24 hours to evaporate the remaining GA solution before use.

2. Determination of the Physical Properties of the Constructed CS/OA Nanofibers

The viscosity of the CS/OA solutions for electrospinning was measured with a rotational viscometer (Rheolab QC; Anton Paar GmBH, Austria) after the samples were prepared under settled conditions. The viscosity (η) was estimated at the Newtonian plateau section in the viscosity-shear stress curve after performing the Carreau-Yasuda model fitting [28,29]. After the preparation of the CS/OA fibers, the morphological changes of the CS/OA fibers were analyzed by field-emission scanning electron microscopy (SEM) (SNE-4500 M; Daeduk image Inc., South Korea) at an accelerating voltage of 20-30 kV after gold sputtering to surface coat the samples. Each fiber's average diameter was measured by observing the obtained SEM image with ImageJ (National Institutes of Health, Maryland, USA) [30]. The mechanical properties of the fibers were measured through a universal testing machine (Instron Ltd., MA, USA) with a 10 N cell after preparing the sample into a rectangular shape (25 mm×10 mm). The wettability of the fibers was determined by measuring contact angles of water droplets on the electrospun fiber after applying 10 μL of water for 60 seconds.

3. *In vitro* Cell Culture Study

For the cell culture experiments, the electrospun nanofibers were exposed to UV radiation for at least 2 h and washed thrice for 30 min with phosphate-buffered saline (PBS) before cell seeding. A mouse preosteoblast cell line, MC3T3-E1 (Sigma-Aldrich Inc., MA, USA), was cultured in minimal essential medium-alpha (MEM-α; HyClone Inc., UT, USA) supplemented with 10% fetal bovine serum (FBS; HyClone) and 1% penicillin/streptomycin (HyClone) at 37 °C in a humidified atmosphere of 5% CO_2 and 95% air. The subconfluent cells were detached using 0.25% trypsin-EDTA (HyClone), and the viable cells were counted with a trypan blue assay. The cells were seeded onto electrospun nanofibers that were placed in a 24-well plate at a density of 5×10^4 cells per well and then cultured for further analysis. The morphology and viability of the cells were imaged with a live cell staining kit (Invitrogen, CA, USA). After each day of cell seeding, live cells were stained with 2 μM calcein AM (green) for 30 min; the stained images were then observed by a fluorescence microscope (Olympus CO., Japan). To assess cell adhesion and proliferation on different nanofibers, relative cell numbers were determined by directly counting the cells on the acquired images. Similarly, an embryo fibroblast model cell line, NIH3T3 (Thermo Fisher Scientific Inc., UK), was cultured in Dulbecco's modified Eagle's medium (DMEM; PAN Biotech LLC., Germany) supplemented with an addition of 10% (v/v) bovine serum (FBS), 2% (v/v) antibiotics (penicillin/streptomycin), and 1% (v/v) l-glutamine (Sigma-Aldrich) in a humidified atmosphere of 5% CO_2 and 95% air. The SEM images of NIH3T3 cells were analyzed with the same experimental procedure as previously described [31]. The proliferation of NIH3T3 cells was analyzed by using CellTiter 96 AQueous One Solution Cell Proliferation Assay kits (Promega Co., WI, USA) that follow procedures as a multiplate reader when there is an absorbance measurement at 490 nm (Molecular Devices LLC., CA, USA).

RESULTS AND DISCUSSION

1. Preparation of CS/OA Blended Electrospun Nanofibers with High Spinnability and a Homogeneous Fiber Network

The fabrication of pristine CS nanofibers proved challenging due

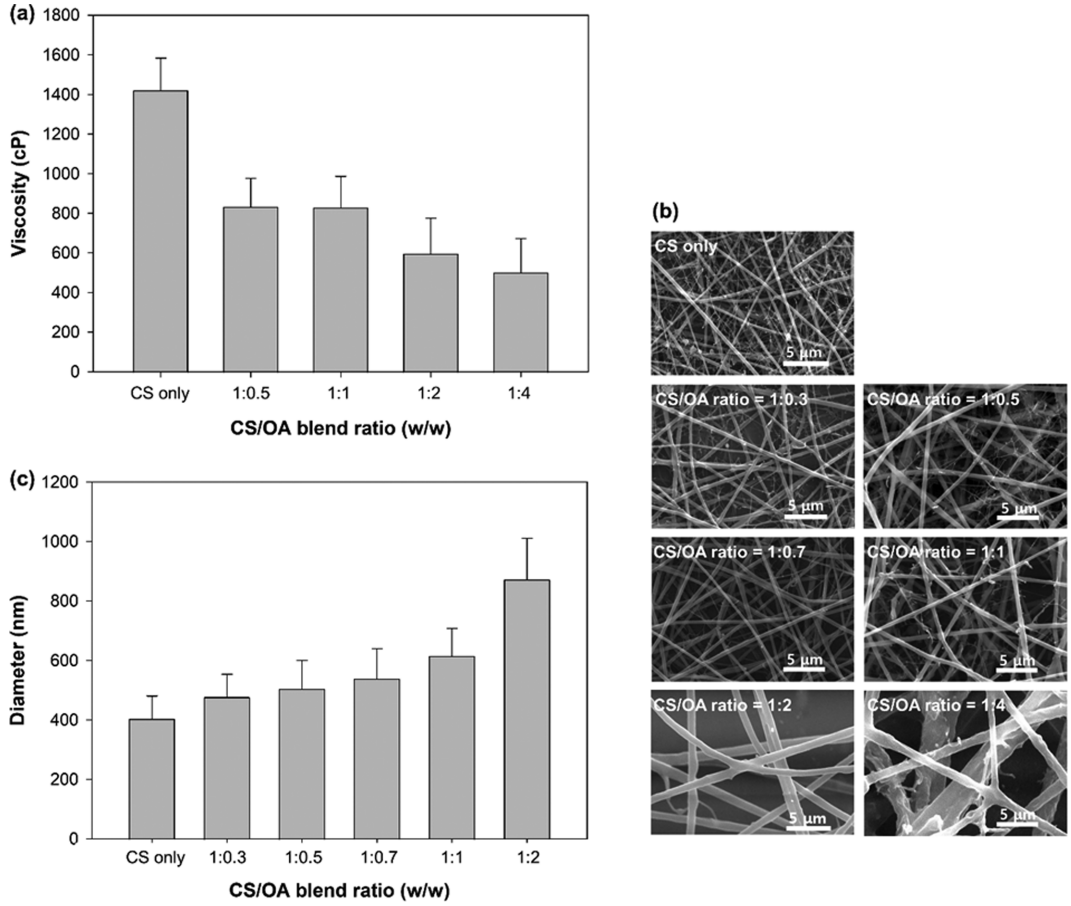

Fig. 1. (a) Viscosities of various solutions of CS/OA blends with different CS/OA ratios. (b) SEM images of CS/OA blended electrospun nanofibers with different CS/OA ratios. (c) Fiber diameters of CS/OA blended electrospun nanofibers with different CS/OA ratios.

to the unfavorably high viscosity in electrospinning solution and the increased polymer jet instability from the strong repulsive forces of NH_3^+ in the CS chains, although the electrospinning process had been optimized by acidic solvents, such as TFA, HFIP, and acetic acid [19,32,33]. In our experiments, the apparent viscosity of our CS nanofiber solution was 1,418.9±164.3 cP (Fig. 1(a)). The electrospinning process in the CS solution was also not stable to prepare a homogeneous fiber network, although electrospun CS fibers could be obtained initially. Some beads were observed in the electrospun nanofiber using the CS-only sample (Fig. 1(b)), which was conventionally reported in other previous studies [34]. The solution viscosity combined with appropriate conductivity had to be within a certain window for successful nanofiber fabrication, and the high viscosity above 1,500 cP could cause spinning jet failure in the CS nanofiber [32,35]. In this manner, we applied OA as a blending compound to improve the solution properties for the electrospinning process. OA derived from the oleic acid is hydrophobic as a fatty acid primary amide and acts as a lubricating agent with bactericidal properties [26,27], which might adjust the strong hydrogen bonds and viscosity in the chitosan solution for electrospinning. In our experiments, the addition of OA to the CS solution significantly decreased the viscosity; the apparent viscosities of the CS/OA mixtures with ratios of 1 : 0.5 and 1 : 4 were 833.62± 142.83 cP and 500.63±171.27 cP, respectively; the increased OA ratio gradually decreased the viscosity (Fig. 1(a)). The reduced viscosity could improve the spinnability to prepare homogeneous fiber networks [35]. Electrospun fibers made from the CS/OA blend solutions were well deposited without bead formation and well accumulated on the bottom of the system for various CS/OA blend ratios. Fig. 1(b) shows the SEM images of the morphology of the electrospun CS/OA fibers. Interestingly, although the addition of OA decreased the solution viscosity, the increased proportion of OA increased the diameter of the electrospun fibers (Fig. 1(c)). However, a microfiber mat with a nonuniform diameter was obtained in a 1 : 4 ratio of CS/OA (Fig. 1(b)). The polymer concentration increased with OA content, and the reduced ratio of CS in the CS/OA blend could decrease the conductivity and charge density on the surface of the drop formed in the needle, resulting in an increased fiber diameter; similar results were also shown in the nanofiber fabrication by blending chitosan with other synthetic polymers such as polycaprolactone and polyethylene oxide [32,36,37]. Overall, the addition of OA to the CS solution enhanced the spinnability, and pristine electrospun nanofibers were successfully obtained in our experiments.

2. Wettability and Mechanical Properties of CS/OA Blended Electrospun Nanofibers

The wettability of CS/OA nanofibers, which measures surface hydrophobicity, was investigated by determining the water contact

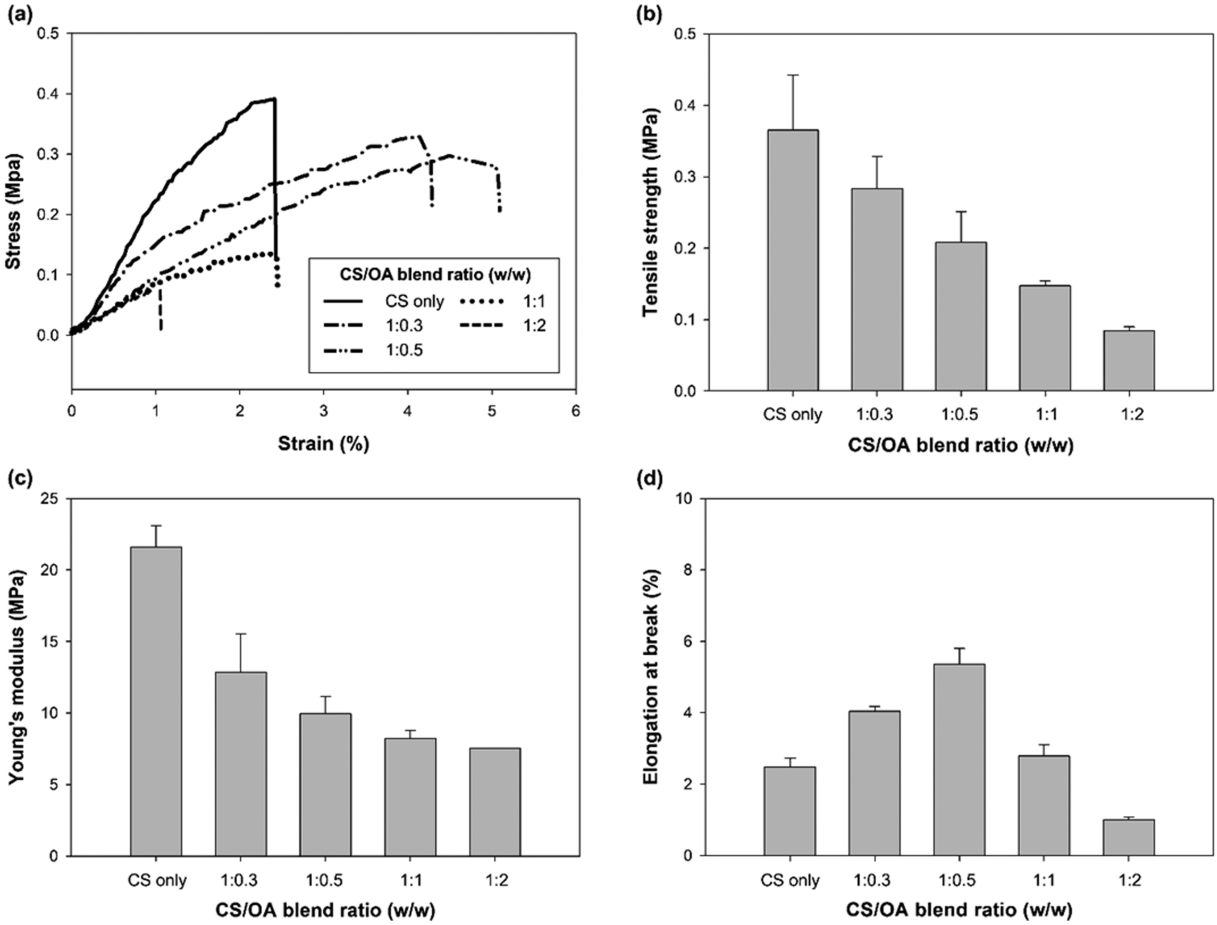

Fig. 2. Mechanical properties of CS/OA blended electrospun nanofibers with different CS/OA ratios. (a) Tensile stress-strain curves. (b) Tensile strength. (c) Young's modulus. (d) Elongation at break.

angle. In the CS-only nanofiber, the water instantly penetrated the CS nanofiber mat. The 1 : 0.3 ratio of the CS/OA nanofiber mat was slowly wetted; thus, the water contact angles were not determined in these samples. However, a further increase in the CS/OA ratio to 1 : 0.5 resulted in a water contact angle of 86.63°; the water contact angle was 90.67° in the 1 : 1 ratio and 96.69° in the 1 : 2 ratio. The increased amount of OA in the CS/OA blended nanofiber gradually increased the hydrophobicity, enabling the construction of nanofiber mats with moderately hydrophobic surfaces compared to hydrophilic CS nanofibers.

Mechanical properties, such as tensile strength, Young's modulus, and elongation at break, of the nanofiber mats were investigated from the tensile stress-strain curves of the CS/OA blended nanofibers (Fig. 2). The tensile strength and Young's modulus decreased with increasing OA content (Fig. 2(b) & (c)). However, the elongation at break first increased and then decreased with increasing OA amount (Fig. 2(d)). The addition of OA could weaken the intermolecular hydrogen bonding network in CS; however, the diameter of the nanofiber increased with increasing OA content. A certain amount of OA in the CS/OA blend that acted as a lubricant could decrease the mechanical stiffness and increase the low elasticity of the CS nanofiber. Additionally, low mechanical strength was obtained in other CS-based porous membranes; these mechanical properties suggested the potential applicability of CS-based nanofibers for wound dressing/healing and drug delivery materials [38, 39]. Moreover, both CS and OA have antibacterial properties preventing bacterial penetration into the skin, and hydrophobic nanofibers can control moisture evaporation from hydrated surfaces, such as wound sites [27,40,41]. From these characteristics, we expect that the CS/OA nanofiber mat might be applicable as a potential wound dressing biomaterial.

3. *In vitro* Cell Adhesion and Proliferation

We investigated *in vitro* cell adhesion and proliferation abilities on the CS/OA blended nanofiber mats with two mouse model cell lines: preosteoblast MC3T3-E1 and fibroblast NIH/3T3. To begin, MC3T3-E1 cells were similarly attached in the CS-only and 1 : 0.5 ratio of CS/OA blended nanofiber surface with extended morphology for 3 days (Fig. 3(a) and (b)), indicating that the CS/OA nanofiber with high spinnability can also be applicable for the *in vitro* cell culture. However, the proliferation levels decreased with increasing OA content (Fig. 3(c)). In addition, the growth seemed unfavorable in the 1 : 1 and 1 : 2 ratios of CS/OA nanofiber mats, where the relative cell numbers significantly decreased with the increased OA ratio. Additionally, cells with round morphology were observed and lost contact with the surfaces in the 1 : 1 and 1 : 2 ratios of CS/OA nanofiber mats, which are some typical morpho-

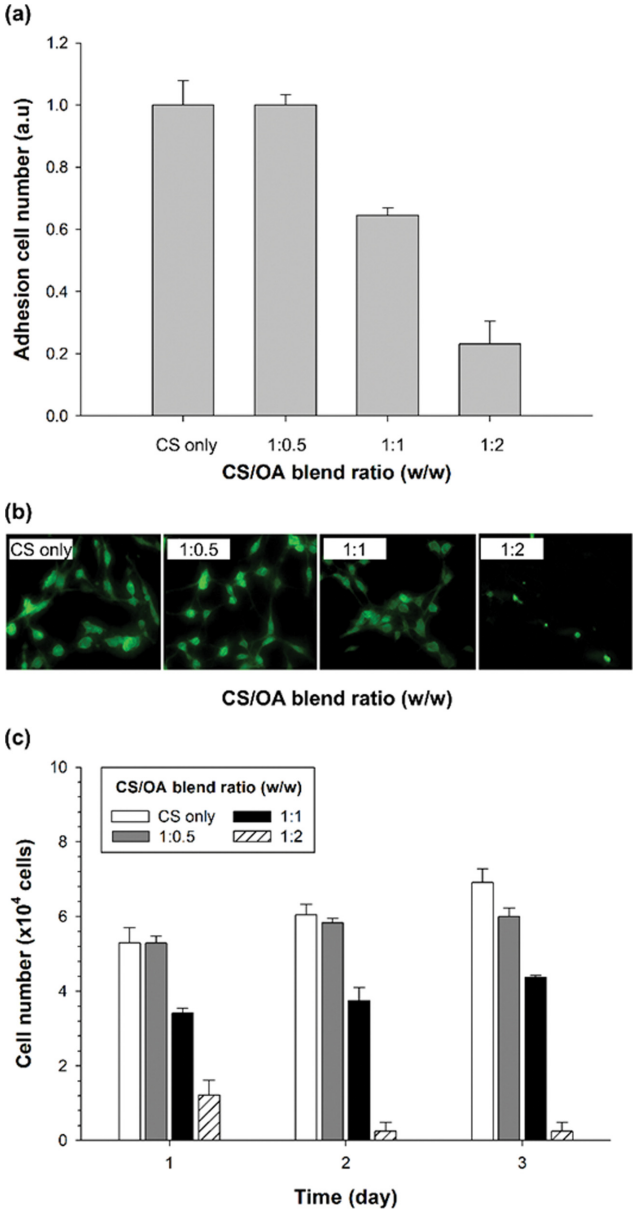

Fig. 3. Cell adhesion (a), morphology (b), and proliferation (c) of MC3T3-E1 cells on CS/OA blended electrospun nanofibers with different CS/OA ratios.

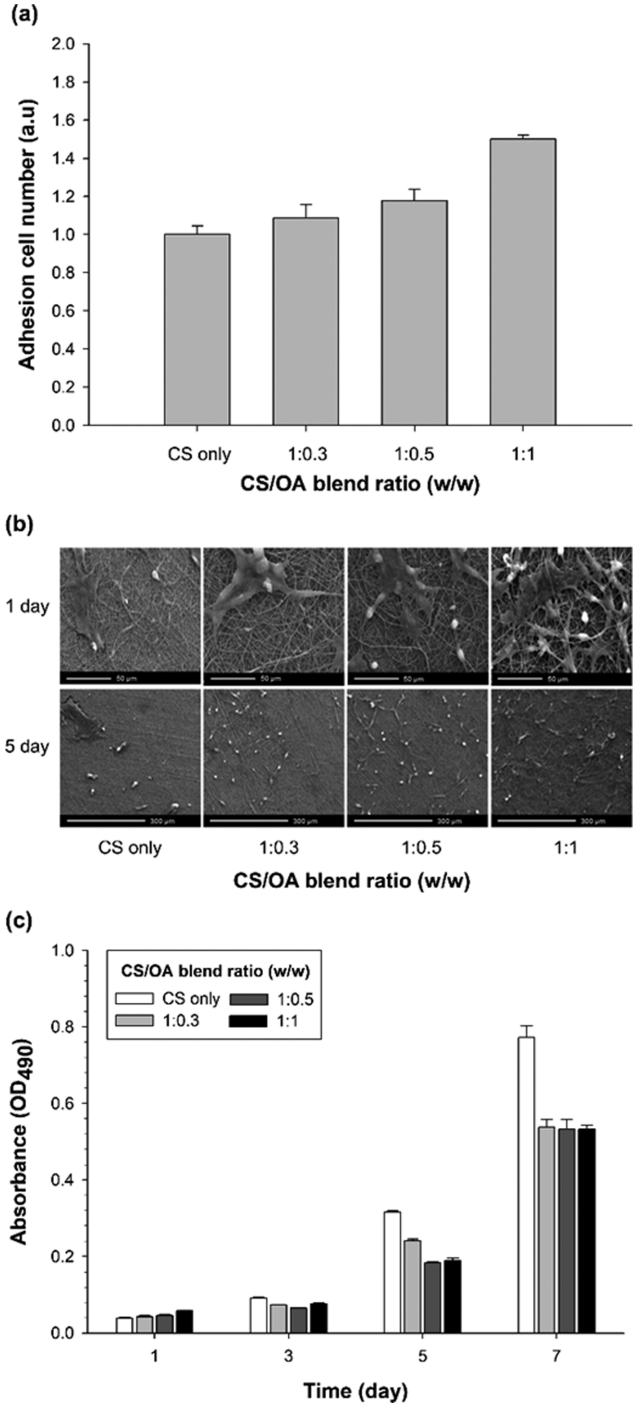

Fig. 4. Cell adhesion (a), morphology (b), and proliferation (c) of NIH/3T3 cells on CS/OA blended electrospun nanofibers with different CS/OA ratios.

logical changes of apoptosis [42]. Because of the importance of mammalian cell spreading events, the blended nanofibers with CS/OA ratios above 1 : 1 seemed to be unavailable for *in vitro* cell culture due to the unfavorable cell attachment environment and poor, round-shaped spreading morphology. Relatively rough and hydrophilic surfaces are typically more attractive to the cell adhesion of osteogenic cells [43,44]. Increased hydrophobicity might hamper cell attachment and proliferation in osteogenic MC3T3-E1 cells [45].

Next, cell adhesion and proliferation were investigated in mouse fibroblast NIH/3T3 cells. Unlike MC3T3-E1 cells, NIH/3T3 cells exhibited higher adhesion ability on the CS/OA nanofiber surfaces; the attached cell numbers were increased to 1.09, 1.18, and 1.5-fold in the 1 : 0.5-, 1 : 0.7-, and 1 : 1-ratio of CS/OA nanofibers, respectively, compared to the CS nanofiber surface (Fig. 4(a)). Relatively smooth and hydrophobic surfaces can be more appropriate than osteogenic cells for seeding fibroblasts and endothelial cells [43,44]. Additionally, cell spreading behavior seemed similar in all samples at the initial stage (Fig. 4(b)). However, after three days, the proliferation level on the CS-only nanofiber was also higher than that

on the CS/OA blended nanofibers, although the proliferation levels on the CS/OA nanofibers were similar regardless of the CS/OA ratio (Fig. 4(c)). For NIH/3T3 cells, cell adhesion and growth were greater on moderately hydrophobic materials at the initial stage, but cell proliferation over long culture periods could be more favorable on hydrophilic surfaces [46].

CONCLUSION

A pristine CS-based electrospun nanofiber was constructed by blending OA with CS. The addition of the fatty acid amide OA moderately decreased the viscosity of the electrospinning solution, resulting in enhanced spinnability for CS/OA blended nanofiber fabrication. The CS/OA nanofibers exhibited moderate hydrophobicity with a water contact angle of approximately 90°. Remarkably, the 1 : 0.5 ratio of CS/OA nanofiber showed relatively high elongation at break, although the increased OA ratio decreased the tensile strength and Young's modulus, as seen in the strain-stress curves. *In vitro* cell culture using NIH/3T3 as a model fibroblast revealed that the CS/OA nanofibers had higher cell adhesion at the early stages than the CS-only nanofiber. Overall, we efficiently obtained CS/OA nanofibers with enhanced spinnability. By considering the mechanical properties and *in vitro* cell culture of the CS/OA nanofiber, it was found that this nanofiber might be applicable as a biomaterial for wound dressing membranes or patches that have intrinsic antibacterial properties and moderate hydrophobicity.

ACKNOWLEDGEMENTS

This work was supported by the National Research Foundation of Korea (NRF-2020R1I1A3072957) funded by the Ministry of Science and ICT, Korea, and by Korea Institute of Marine Science & Technology Promotion (KIMST) funded by the Ministry of Oceans and Fisheries, Korea (20220532).

REFERENCES

1. J. J. Xue, T. Wu, Y. Q. Dai and Y. N. Xia, *Chem. Rev.*, **119**, 5298 (2019).
2. S. Asghari, F. Barati, M. Avatefi and M. Mahmoudifard, *Biotechnol. Bioprocess Eng.*, **26**, 529 (2021).
3. M. S. Islam, A. Andriyana, A. M. Afifi and B. C. Ang, *SN Appl. Sci.*, **1**, 1248 (2019).
4. X. Y. Yin, Y. Q. Wang, H. Yu, Y. X. Gao, Y. He and J. Y. Chen, *Korean J. Chem. Eng.*, **37**, 1751 (2020).
5. D. I. Braghirolli, D. Steffens and P. Pranke, *Drug Discov. Today*, **19**, 743 (2014).
6. C. P. Barnes, S. A. Sell, E. D. Boland, D. G. Simpson and G. L. Bowlin, *Adv. Drug Deliv. Rev.*, **59**, 1413 (2007).
7. A. D. Theocharis, S. S. Skandalis, C. Gialeli and N. K. Karamanos, *Adv. Drug Deliv. Rev.*, **97**, 4 (2016).
8. J. Rnjak-Kovacina, F. Tang, J. M. Whitelock and M. S. Lord, *Adv. Healthc. Mater.*, **7**, e1701042 (2018).
9. C. Frantz, K. M. Stewart and V. M. Weaver, *J. Cell Sci.*, **123**, 4195 (2010).
10. M. Keshvardoostchokami, S. S. Majidi, P. P. Huo, R. Ramachandran, M. L. Chen and B. Liu, *Nanomaterials*, **11**, 21 (2021).
11. T. Abudula, H. S. Mohammed, K. Joshi Navare, T. Colombani, A. Memic and S. A. Bencherif, *ACS Appl. Bio Mater.*, **2**, 952 (2019).
12. A. M. Afifi, H. Jahangirian, T. J. Webster and K. Kalantari, *Carbohydr. Polym.*, **207**, 588 (2019).
13. R. LogithKumar, A. KeshavNarayan, S. Dhivya, A. Chawla, S. Saravanan and N. Selvamurugan, *Carbohydr. Polym.*, **151**, 172 (2016).
14. P. P. Feng, Y. Luo, C. H. Ke, H. F. Qiu, W. Wang, R. X. Hou, L. Xu, S. Z. Wu and Y. B. Zhu, *Front. Bioeng. Biotechnol.*, **9**, 650598 (2021).
15. A. D. Baldwin and K. L. Kiick, *Pept. Sci.*, **94**, 128 (2010).
16. R. V. Kumaraswamy, S. Kumari, R. C. Choudhary, A. Pal, R. Raliya, P. Biswas and V. Saharan, *Int. J. Biol. Macromol.*, **113**, 494 (2018).
17. Z. Zhang, F. J. Jin, Z. C. Wu, J. Jin, F. Li, Y. L. Wang, Z. P. Wang, S. Q. Tang, Y. F. Wang and C. X. Wu, *Carbohydr. Polym.*, **177**, 203 (2017).
18. H. Homayoni, M. Valizadeh and S. A. H. Ravandi, *Carbohydr. Polym.*, **77**, 656 (2009).
19. A. Pérez-Nava, E. Reyes-Mercado and J. B. González-Campos, *Chem. Eng. Process.*, **173**, 108849 (2022).
20. D. Cha, H. Kim, A. Nishida, H. Yamamoto and K. Ohkawa, *Macromol. Rapid Commun.*, **25**, 1600 (2004).
21. F. Seidi, M. K. Yazdi, M. Jouyandeh, M. Dominic, H. Naeim, B. Bagheri, S. Habibzadeh, P. Zarrintaj, M. R. Saeb, M. N. Nezhad and M. Mozafari, *Int. J. Biol. Macromol.*, **183**, 1818 (2021).
22. S. Mohebbi, P. Zarrintaj, S. H. Jafari, S. S. Gholizadeh, M. N. Nezhad, M. R. Saeb and M. Mozafari, *Curr. Stem Cell Res. Ther.*, **14**, 93 (2019).
23. A. H. Rather, T. U. Wani, R. S. Khan, B. Pant, M. Park and F. A. Sheikh, *Int. J. Mol. Sci.*, **22**, 4017 (2021).
24. S. Datta, A. P. Rameshbabu, K. Bankoti, P. P. Maity, D. Das, S. Pal, S. Roy, R. Sen and S. Dhara, *ACS Biomater. Sci. Eng.*, **3**, 1738 (2017).
25. E. Kang, E. Moon, W. Song, L. H. Kim, J. S. Hyung, J.-H. Jo, J.-H. Park, M.-S. Kim, J.-G. Na and Y. S. Choi, *Chem. Eng. J.*, **433**, 133846 (2022).
26. P. Getachew, M. Getachew, J. Joo, Y. S. Choi, D. S. Hwang and Y.-K. Hong, *Toxicol. Environ. Health Sci.*, **8**, 341 (2016).
27. E. Seo, M. R. Seong, J. W. Lee, H. Lim, J. Park, H. Kim, H. Hwang, D. Lee, J. Kim, G. H. Kim, D. S. Hwang and S. J. Lee, *ACS Omega*, **5**, 11515 (2020).
28. E. Brunengo, M. Alloisio, A. Sionkowska, S. Vicini, A. Dodero and M. Castellano, *Carbohydr. Polym.*, **235**, 115976 (2020).
29. K. Yasuda, R. C. Armstrong and R. E. Cohen, *Rheol. Acta.*, **20**, 163 (1981).
30. K. Bharti, H. Kriel, C. G. Simon, Jr. and N. A. Hotaling, *Biomaterials*, **61**, 327 (2015).
31. E. Kang, H. H. Je, E. Moon, J.-G. Na, M. S. Kim, D. S. Hwang and Y. S. Choi, *Carbohydr. Polym.*, **258**, 117733 (2021).
32. R. R. Klossner, H. A. Queen, A. J. Coughlin and W. E. Krause, *Biomacromolecules*, **9**, 2947 (2008).
33. B. S. de Farias, T. R. S. Cadaval and L. A. D. Pinto, *Int. J. Biol. Macromol.*, **123**, 210 (2019).
34. H. F. Naguib, R. E. Morsi and M. Z. Elsabee, *Mater. Sci. Eng. C-Mater. Biol. Appl.*, **32**, 1711 (2012).
35. K. I. Minato, G. Kumagai, S. Hayashi, H. Yamamoto and K. Ohkawa, *Biomacromolecules*, **7**, 3291 (2006).
36. A. C. Areias, V. Sencadas, J. Alio, J. L. G. Ribelles, S. Lanceros-Mendez and J. A. Gomez-Tejedor, *Polym. Eng. Sci.*, **52**, 1293 (2012).

37. L. V. der Schueren, I. Steyaert, B. D. Schoenmaker and K. D. Clerck, *Carbohydr. Polym.*, **88**, 1221 (2012).
38. A. P. Rodrigues, E. M. S. Sanchez, A. C. da Costa and A. M. Moraes, *J. Appl. Polym. Sci.*, **109**, 2703 (2008).
39. C. Z. Bueno and A. M. Moraes, *J. Appl. Polym. Sci.*, **122**, 624 (2011).
40. K. S. Ogueri and C. T. Laurencin, *ACS Nano.*, **14**, 9347 (2020).
41. C. X. Wu, T. Chen, Y. J. Xin, Z. Zhang, Z. Ren, B. Chu, Y. F. Wang, J. Lei and S. Q. Tang, *Biomed. Mater.*, **11**, 035019 (2016).
42. G. V. Kulkarni and C. A. G. Mcculloch, *J. Cell Sci.*, **107**, 1169 (1994).
43. T. T. Yu, F. Z. Cui, Q. Y. Meng, J. Wang, D. C. Wu, J. Zhang, X. X. Kou, R. L. Yang, Y. Liu, Y. S. Zhang, F. Yang and Y. H. Zhou, *ACS Biomater. Sci. Eng.*, **3**, 1119 (2017).
44. F. Yang, S. Wang, S. Ramakrishna and C. Xu, *J. Biomed. Mater. Res. Part A.*, **71**, 154 (2004).
45. Y. Zamani, J. Mohammadi, D. O. Visscher, M. N. Helder, B. Zandieh-Doulabi, J. Klein-Nulend and G. Amoabediny, *Biomed. Mater.*, **14**, 015008 (2019).
46. E. Torres, A. Vallés-Lluch, B. Napiwocki, T. Lih-Sheng and V. Fombuena, *Macromol. Mater. Eng.*, **302**, 1700259 (2017).